Available online at www.sciencedirect.com
SCIENCE DIRECT
Bioorganic & Medicinal Chemistry 14 (2006) 5666–5672
Bioorganic & Medicinal Chemistry

# Synthesis and high-throughput evaluation of triskelion uracil libraries for inhibition of human dUTPase and UNG2

Yu Lin Jiang, Suhman Chung, Daniel J. Krosky and James T. Stivers*

*Department of Pharmacology and Molecular Sciences, Johns Hopkins University School of Medicine, 725 North Wolfe Street, Baltimore, MD 21205, USA*

Received 22 February 2006; revised 10 April 2006; accepted 13 April 2006
Available online 5 May 2006

**Abstract**—Human nuclear uracil DNA glycosylase (UNG2) and deoxyuridine triphosphate nucleotidohydrolase (dUTPase) are the primary enzymes that prevent the incorporation and accumulation of deoxyuridine in genomic DNA. These enzymes are desirable targets for small molecule inhibitors given their roles in a wide range of biological processes ranging from chromosomal rearrangements that lead to cancer, viral DNA replication, and the formation of toxic DNA strand breaks during anticancer drug therapy. To accelerate the discovery of such inhibitors, we have developed a high-throughput approach for directed library synthesis and screening. In this efficient technology, a uracil-aldehyde ligand is covalently tethered to one position of a trivalent alkyloxyamine linker via an oxime linkage, and then the vacant linker positions are derivatized with a library of aldehydes. The resulting triskelion oximes were directly screened for inhibitory activity and the most potent of these showed micromolar binding affinities to UNG2 and dUTPase.


## 1. Introduction

From the classic view of DNA repair and mutagenesis, the uracil base has no place in genomic DNA.[1] Accordingly, elaborate DNA repair mechanisms have evolved to exclude dUTP from the nucleotide pool used for DNA replication,[5,6] and to remove uracil from DNA when it arises from spontaneous deamination of cytosine bases.[7] However, the uracil base has recently been found to play a much more diverse role in human biology, disease, and anticancer therapy (Fig. 1). Surprisingly, the uracil excision repair machinery has been found to participate in the process of generating somatic mutations during antibody maturation in B cells,[8–10] and uracil incorporation and/or removal is critical in the life cycles of herpes,[11] cytomegalo,[12] pox,[13,14] and type 1 human immunodeficiency viruses (HIV-1).[15] Furthermore, this pathway also generates the pharmacologically active single and double strand DNA breaks that are the essential tumor killing lesions produced by the widely used anticancer drugs 5-fluorouracil and methotrexate,[16,17] and generates the characteristic chromosomal translocations found in some B cell lymphomas. Thus, pharmacologic agents that inhibit these processes are desirable for both investigational and therapeutic purposes.

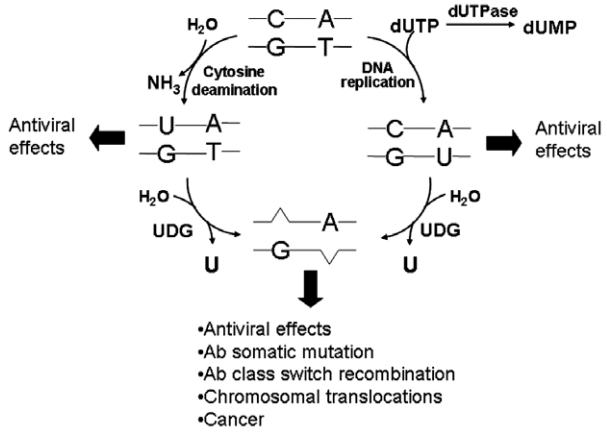


**Figure 1.** Biological effects of uracil in DNA.[2–4]

Human nuclear uracil DNA glycosylase (UNG2) and deoxyuridine triphosphate nucleotidohydrolase

*Keywords*: Uracil DNA glycosylase; dUTPase; Enzyme inhibition; Directed chemical libraries; High-throughput screening.
* Corresponding author. Tel.: +1 410 502 2758; fax: +1 410 955 3023; e-mail: jstivers@jhmi.edu

0968-0896/$ - see front matter © 2006 Elsevier Ltd. All rights reserved.
doi:10.1016/j.bmc.2006.04.022

(dUTPase) are the primary enzymes that prevent the incorporation and accumulation of deoxyuridine in genomic DNA.[17,18] Given that these enzymes are emerging as interesting pharmacologic targets, we have sought out methods for the rapid and efficient identification of small molecule ligands that can inhibit their activity. One of the most exciting potential applications of UNG2 and dUTPase inhibitors would be as antiretroviral agents. Recent findings have established that HIV-1 specifically packages UNG2 into virus particles via interaction with the virus encoded integrase protein (Int), or perhaps a ternary complex between UNG, Int and the viral Vpr protein.[11,19–26] UNG2 is required for infection of nondividing cells such as macrophages and resting T cells, and virus particles produced from UNG depleted cells are incapable of infecting new target cells.[15,27] Infection of macrophages helps maintain a viral reservoir in the host that is crucial for virus spread to the lymphoid organs and T-helper lymphocytes, and ultimately, AIDS pathogenesis.[21,28] UNG is apparently recruited to minimize uracil incorporation into the viral genome in these cells, which have naturally high levels of dUTP, a good substrate for the viral reverse transcriptase.[29] Inhibition of dUTPase would be expected to further increase dUTP levels in macrophages, resulting in even more uracil misincorporation into the viral genome (Fig. 1). Pharmacologic targeting of a UNG2 and dUTPase is extremely attractive because these targets would not be susceptible to the same high mutagenesis rate and resulting drug resistance as viral encoded proteins.[30] Targeting UNG2 is a viable therapeutic strategy because it is not an essential enzyme. Thus, UNG knock-out mice display no remarkable phenotype, nor do UNG null yeast or human cell lines.[31] Although dUTPase is an essential enzyme in all organisms, it would be expected that rapidly replicating viruses such as HIV-1 would show higher sensitivity than the host, providing a potential therapeutic window.

Herein, we report an integrated high-throughput (HTP) platform for the synthesis and evaluation of uracil-directed small molecule libraries based upon triskelion oxyamine scaffolds. The strategy is to attach a uracil-aldehyde ligand to one or two arms of the triskelion scaffold and then derivatize the vacant position(s) with a random library of aldehydes (RCHO). The uracil moiety is expected to weakly target the fully functionalized compound to the active site rather than irrelevant regions of the enzyme, and the random functional groups can then explore nearby binding pockets resulting in increased affinity over that of the uracil alone. Library compounds are rapidly screened using robust HTP activity assays, from which several inhibitors of UNG2 and dUTPase have been identified.

## 2. Results and discussion

### 2.1. Synthesis of uracil triskelion oxime libraries

We sought an inhibitor development strategy that allowed rapid and economical synthesis of small molecule ligands that explore binding sites near the UNG2 and dUTPase active sites, and which could be used directly in HTP screening applications without purification. One efficient synthesis strategy that meets these criteria is outlined in Schemes 1 and 2. First, a triskelion oxyamine scaffold is synthesized in two steps from tris(hydroxymethyl)methane (Scheme 1). Then the three oxyamine groups are derivatized with a uracil-aldehyde and a library of 215 aldehyde binding elements (RCHO, Table 1) via the formation of stable oxime linkages (Scheme 2).

Each linking reaction is carried out in one well of a 96-well microtiter plate that contains one molar equivalent

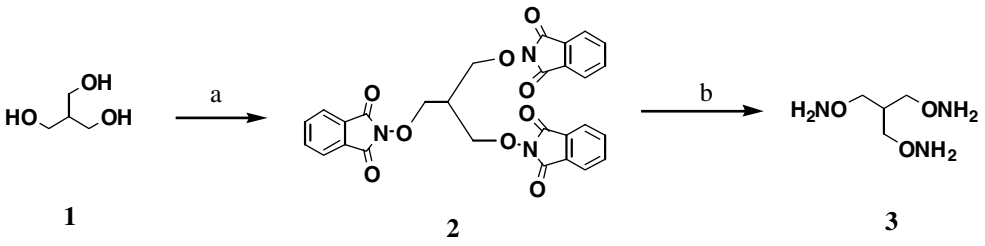


**Scheme 1.** Reagents and conditions: (a) triphenylphosphine, diisopropyl azodicarboxylate, *N*-hydroxyphthalimide, anhydrous THF, overnight, 0 °C, 53% yield; (b) anhydrous $NH_2NH_2$, 95% ethanol, room temperature, 2 h, 67%. See Ref. 32.

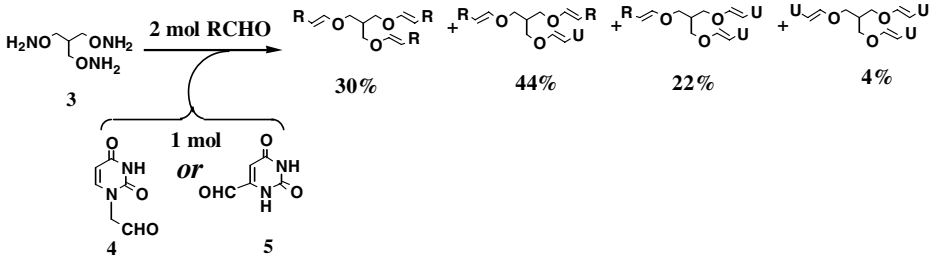


**Scheme 2.** Reagents and conditions: AcOH (20% v/v), DMSO, 12 h, 37 °C.

**Table 1.** Representative aryl aldehydes (RCHO) used in library synthesis[a]

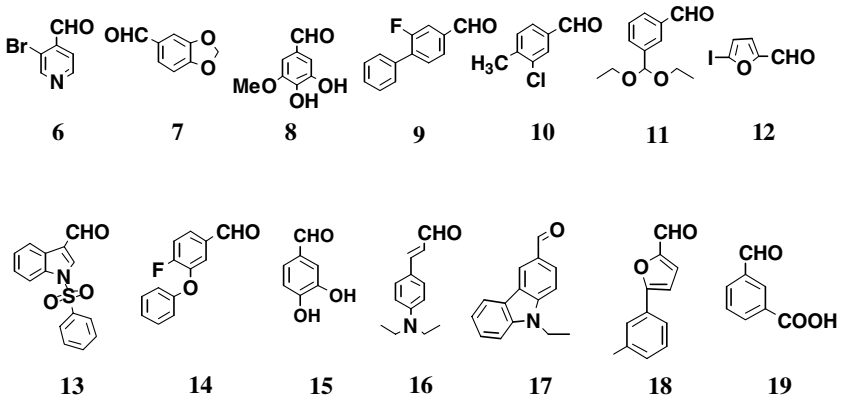


[a] The entire library consisted of 215 aryl aldehydes.

uracil aldehyde, two molar equivalents RCHO library member, and one molar equivalent oxyamine triskelion scaffold (Scheme 2). The reactions typically proceed to 85–99% completion after overnight incubation (DMSO, 37 °C), and produce a statistical mixture of the homotrimeric (UUU, RRR) and heterotrimeric (UUR, RRU) oximes in the approximate amounts indicated in Scheme 2 (see supplemental materials). No compound purification is required before screening the library for active compounds.

### 2.2. High-throughput screening of triskelion libraries against UDG

We have previously developed a high-throughput fluorescence assay for UNG2 that allows screening of chemical libraries.[33] This assay was used to screen the 215 oxime mixtures obtained from reaction of the triskelion oxyamine scaffold with uracil **5** and library aldehydes **6** through **34**. Mixtures that showed inhibitory activity were subjected to fractionation using reversed-phase HPLC, and then the individual purified components were reevaluated to determine which species was responsible for the inhibition. After identifying the inhibitory molecules, they were resynthesized in larger scale, purified, and complete $IC_{50}$ curves were determined as previously described.[33]

Two RCHO groups were found to be inhibitory when attached to uracil in the triskelion scaffold (Table 2). The $IC_{50}$ values were found to fall in the range ~0.9 to 11 μM. When RCHO = 3,4 dihydroxybenzaldehyde, both the RRU (**45**) and UUR (**46**) variants showed nearly equal activity, suggesting that the enzyme recognizes the UR element, but not the third substituent on the scaffold (U or R). Consistent with this interpretation, the corresponding bifunctional oxime (UR, **47**, Table 2)[33] showed a similar $IC_{50}$ value as **45** and **46**. In contrast, when RCHO = 3-carboxybenzaldehyde, the trivalent forms **48** and **49** were found to be 6- to 12-fold more potent than the bifunctional oxime **50**. Thus, in this latter case the third substituent has a significant effect on binding affinity.

### 2.3. High-throughput screening of triskelion libraries against dUTPase

A similar strategy was used to screen the 215 oxime mixtures obtained from reaction of the triskelion scaffold with uracil aldehyde **4** and library aldehydes **6** through **34** against human dUTPase. In this case, only one inhibitory RCHO group was found (Table 3), and both the RRU (**51**) and UUR (**52**) variants provided comparable $IC_{50}$ values in the range 3–5 μM. To the best of our knowledge, **51** and **52** are the most potent nonnucleotide inhibitors of human dUTPase yet reported.

### 2.4. Inhibition by the untethered parts

The key question in determining the effectiveness of this tethering strategy is the inhibitory capacities of the untethered uracil and aldehyde components. For UNG2, the methyl oxime of uracil **5** has an $IC_{50}$ value of 75 μM, and no inhibition by the methyl oxime of 3,4 dihydroxybenzaldehyde (**15**) could be detected even at concentrations as high as 1 mM. Thus, tethering **15**–**5** produced an increase in binding affinity of 75-fold relative to uracil alone, and tethering **5**–**15** brought about at least a 1000-fold increase in binding affinity relative to **15** alone. For dUTPase, the methyl oximes of **4** and **8** were not inhibitory even at concentrations as high as 1 mM. Thus in this case, tethering of the two parts has brought about increases in binding affinity of at least 700-fold as compared to the separate components. A trivial but potentially useful modification of the tethering approach would be to incorporate two different R groups into the triskelion scaffold. This is easily accomplished by first synthesizing and isolating the monoderivatized uracil compound and then reacting the remaining two oxyamine positions with a mixture of two aldehydes (unpublished).

## 3. Conclusion

We have established that triskelion libraries of uracil derivatives can efficiently yield inhibitors with micromolar affinities for two different enzymes that recognize the

**Table 2.** Structures and inhibitory constants for UNG2 inhibitors[a]

| Triskelion compound | $IC_{50}$ (μM) |
|---|---|
| 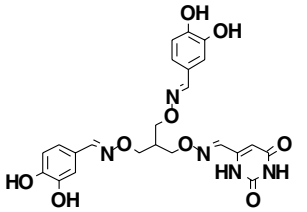 **45** | 1.6 ± 0.1 |
| 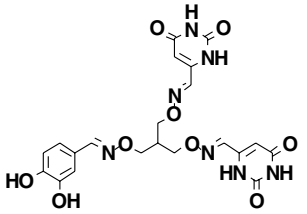 **46** | 0.9 ± 0.1 |
| 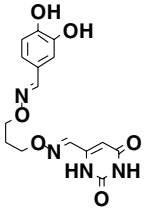 **47** | 1.3 ± 0.1 |
| 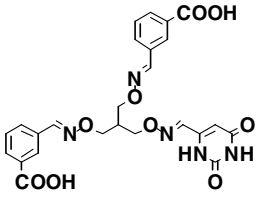 **48** | 1.7 ± 0.5 |
| 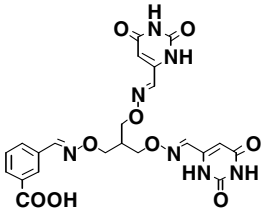 **49** | 0.9 ± 0.1 |
| 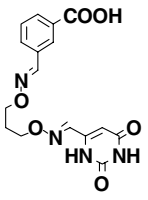 **50** | 10.9 ± 0.5 |

[a] See Ref. 33 for representative HTS screening data and $IC_{50}$ curves.

**Table 3.** Structures and inhibitory constants for dUTPase inhibitors

| Triskelion compound | $IC_{50}$ (μM) |
|---|---|
| 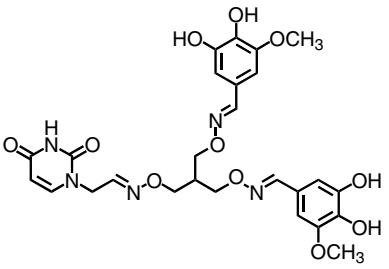 **51** | 3.3 ± 1.1 |
| 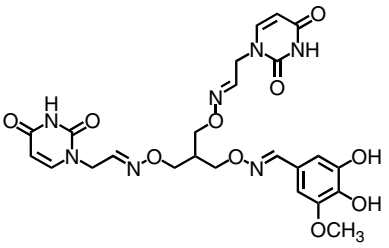 **52** | 5.5 ± 1.0 |

uracil base. Unlike previous nucleic acid-based inhibitors of UNG.[34,35] and nucleotide-based inhibitors of dUTPase,[36] these library compounds are expected to be cell permeable. A useful extension of this approach is currently being developed where the length of the linker arms is varied. This modified approach is expected to generate more diverse libraries that allow more comprehensive probing of potential binding sites near the uracil pocket.

With respect to the in vivo utility of such oxime libraries, there are a number of currently used drugs with oxime functional groups: the selective serotonin reuptake inhibitor, fluvoxamine,[37,38] the monobactam antibiotic, aztreonam,[38] and several preclinical antimicrobial drugs.[39,40] The activity of these drugs indicates that oxime linkages are stable and useful in real clinical applications. Nevertheless, oximes are susceptible to reduction in metabolic reactions involving cytochrome P450-mediated transformations.[40,41] Depending on the pharmacokinetic and pharmacodynamic properties of the individual oximes, this may or may not pose a problem. For instance fluvoxamine, although extensively processed in first-pass metabolism, has a reasonable serum half-life of 12 h.[37,38] We anticipate that triskelion libraries based on substrate fragments will be useful for rapid inhibitor development against a variety of enzymes.

## 4. Experimental

### 4.1. Reagents and general methods

All chemicals were purchased from commercial sources without further purification unless otherwise stated. The $^{1}H$ and $^{13}C$ NMR spectra were recorded on a 400 MHz Varian Innova instrument. The spectra were recorded in deuteriochloroform ($CDCl_3$) or in hexadeu-

teriodimethylsulfoxide (DMSO-$d_6$). The chemical shifts of protons are given in ppm with TMS as internal standard. The chemical shifts of carbons are obtained in ppm with solvents as internal standards. Oximes were purified by HPLC using aqueous triethylammonium acetate (TEAA) as a running buffer. Therefore, TEAA was not completely removed and it appeared in the NMR spectra. Accordingly, proton and carbon chemical shifts of TEAA were not listed during the characterizations of the oximes. During purification of the oximes **45** and **46**, 2-mercaptoethanol was used as an anti-oxidant. Therefore, small amounts of this compound and its oxidation product are also present in these oximes. Flash chromatographies were performed with silica (70–230 mesh from Sorbent Technologies) and monitored by thin-layer chromatography (TLC) with silica plates (Merck, Kieselgel 60 F254).

### 4.2. 2,2′,2″-[(2-Methyloxy-1,3-propanedioxy)tris]-1*H*-isoindole-1, 3(2*H*)-dione (2)

To a suspension of 2-hydroxymethyl-1,3-propanediol **1** (0.848 g, 8.0 mmol), triphenylphosphine (7.32 g, 28 mmol), and *N*-hydroxyphthalimide (6.52 g, 40 mmol) in anhydrous THF (60 ml) was added diisopropyl azodicarboxylate (5.64 ml, 28.0 mmol) dropwise at 0 °C.[42–44] The mixture was stirred overnight, and the precipitate was filtered and washed with cold THF. After removal of the THF in vacuo, product **2** was obtained (2.3 g) in 53% yield. $^1$H NMR (400 MHz, $CDCl_3$): $\delta$ 7.76 (m, 12H), 4.66 (d, $J$ = 6.4 Hz, 6H), 2.78 (septet, $J$ = 6.4 Hz, 1H); $^{13}$C NMR (100 MHz, $CDCl_3$): $\delta$ 163.43, 134.39, 128.97, 123.47, 75.52, 37.68. HRMS (*m*/*z*): $[M+H]^+$ calcd for $C_{28}H_{20}N_3O_9$, 542.12; found, 542.12.

### 4.3. 2-[(Aminooxy)-methyl]-1,3-bis(aminooxy)-propane (3)

To a suspension of **2** (2.43 g, 4.5 mmol) in 95% ethanol (9.5 ml), was added anhydrous hydrazine (0.67 ml, 20.2 mmol) dropwise within 10 min at room temperature. The mixture was stirred for 2 h, filtered, and washed with 95% ethanol. The filtrate was concentrated in vacuo to give a residue. To the residue was added methylene chloride (10 ml). The resulting mixture was kept overnight at room temperature, filtered the following morning, and the filtrate was concentrated in vacuo, giving product **3** (0.46 g) in 67% yield. $^1$H NMR (400 MHz, $CDCl_3$): $\delta$ 3.71 (d, $J$ = 6.0 Hz, 6H), 2.41 (septet, $J$ = 6.4 Hz, 1H); $^{13}$C NMR (100 MHz, $CDCl_3$): $\delta$ 74.66, 37.05; HRMS (*m*/*z*): $[M+H]^+$ calcd for $C_4H_{14}N_3O_3$, 152.10; found, 152.10.

### 4.4. General synthesis of tethered triskelion oximes

A set of 39 commercially available aldehydes were linked to the two uracil-containing aldehydes **4** and **5** using the triskelion alkyloxyamine linker **3** (see Scheme 2 and Table 1, and supplementary materials). To each well of a 0.5-ml Matrix microtiter plate were added DMSO stock solutions of AcOH (20 μL, 150 mM, 3 μmol), uracil-containing aldehyde **4** or **5** (20 μL, 150 mM, 3 μmol), and one library aldehyde (40 μL, 150 mM, 6 μmol). The synthesis and characterization of **4** and **5** has been previously reported. The plate was carefully agitated to make the solutions homogeneous, and 22 μL of a DMSO solution of the triskelion oxyamine was then added (150 mM, 3.3 μmol). The plate was sealed and further agitated and incubated in an oven for 12 h at 37 °C. The expected statistical ratios of the oxime products were confirmed by $^1$H NMR analysis (see supplementary materials).

### 4.5. Isolation and purification of inhibitory triskelion oximes

The most potent inhibitors were resynthesized in larger scale and thoroughly characterized after HPLC purification of the mixed oximes using a Phenomenex Aqua reversed-phase C-18 HPLC column (250 mm, 10 mm, 5 μm). Gradient elution from 0% to 65% $CH_3CN$ in 0.1 M aqueous TEAA over the course of 2 h with UV detection at 254 nm was used. An exception was oxime **47**, which is prone to air oxidation. In this case, 25 mM 2-mercaptoethanol was added to both of the running buffers. The oximes all eluted with baseline resolution in the order (1) the homotrimer oxime derived from **4** or **5**, (2) the heterotrimer oxime derived from **4** or **5** and either **8**, **15** or **19**, and (3) the homotrimer oxime derived from **8**, **15** or **19**.

### 4.6. 2-[*O*-(6-Uracilcarboxaldoximyl)-methyl]-1,3-bis[*O*-(3,4-dihydroxybenzaldoximyl)]-propane (45)

$^1$H NMR (400 MHz, DMSO-$d_6$): $\delta$ 11.15 (br s, 1H), 9.30 (br s, 1H), 8.09 (s, 2H), 7.98 (s, 1H), 7.05 (d, $J$ = 1.6 Hz, 1H), 6.84 (dd, $J$ = 8.0, 2.0 Hz, 1H), 6.74 (d, $J$ = 8.0 Hz, 1H), 5.78 (s, 1H), 4.32 (d, $J$ = 6.0 Hz, 2H), 4.17 (d, $J$ = 5.6 Hz, 4H), 2.66 (m, 1H); $^{13}$C NMR (100 MHz, DMSO-$d_6$): $\delta$ 163.85, 151.04, 149.12, 147.70, 145.57, 144.51, 142.43, 123.09, 119.95, 115.60, 112.91, 101.78, 73.25, 71.13, 38.67; HRMS (*m*/*z*): $[M+H]^+$ calcd for $C_{23}H_{24}N_5O_9$, 514.16; found, 514.16.

### 4.7. 2-[*O*-(3,4-Dihydroxybenzaldoximyl)-methyl]-1,3-bis[*O*-(6- uracilcarboxaldoximyl)]-propane (46)

$^1$H NMR (400 MHz, DMSO-$d_6$): $\delta$ 11.15 (br s, 1H), 8.05 (s, 1H), 7.97 (s, 2H), 7.04 (d, $J$ = 2.0 Hz, 1H), 6.84 (dd, $J$ = 8.0, 2.0 Hz, 1H), 6.74 (d, $J$ = 8.0 Hz, 1H), 5.78 (s, 2H), 4.32 (d, $J$ = 6.4 Hz, 4H), 4.16 (d, $J$ = 6.0 Hz, 2H), 2.66 (m, 1H); $^{13}$C NMR (100 MHz, DMSO-$d_6$): $\delta$ 164.50, 151.72, 149.84, 148.39, 146.24, 145.16, 143.13, 123.68, 120.61, 116.25, 113.61, 102.40, 73.73, 71.60, 38.98; HRMS (*m*/*z*): $[M+H]^+$ calcd for $C_{21}H_{22}N_7O_9$, 516.15; found, 516.15.

### 4.8. 1-[*O*-(6-Uracilcarboxaldoximyl)]-3-[*O*-(3,4-dihydroxybenzaldoximyl)]-propane (47)

The synthesis and characterization of this oxime heterodimer has been previously described[33].

### 4.9. 2-[*O*-(6-Uracilcarboxaldoximyl)-methyl]-1,3-bis[*O*-(3-carboxybenzaldoximyl)]-propane (48)

$^1$H NMR (400 MHz, DMSO-$d_6$): $\delta$ 8.34 (s, 2H), 8.15 (s, 2H), 8.0 (s, 1H), 7.91 (d, $J$ = 6.8 Hz, 2H), 7.65 (d,

$J$ = 8.0 Hz, 2H), 7.38 (t, $J$ = 8.4 Hz, 2H), 5.77 (s, 1H), 4.36 (d, $J$ = 6.4 Hz, 2H), 4.28 (d, $J$ = 5.6 Hz, 4H), 2.82 (m, 1H); $^{13}$C NMR (100 MHz, DMSO-$d_6$): $\delta$ 168.54, 163.88, 151.07, 149.16, 144.57, 142.60, 137.36, 131.43, 130.62, 128.75, 128.27, 127.55, 101.86, 73.12, 71.50, 38.67; HRMS (*m*/*z*): $[M+H]^+$ calcd for $C_{25}H_{24}N_5O_9$, 538.16; found, 538.16.

### 4.10. 2-[*O*-(3-Carboxybenzaldoximyl)-methyl]-1,3-bis[*O*-(6-uracilcarboxaldoximyl)]-propane (49)

$^1$H NMR (400 MHz, DMSO-$d_6$): $\delta$ 11.17 (br s, 1H), 8.32 (s, 1H), 8.16 (s, 1H), 8.0 (s, 2H), 7.92 (dd, $J$ = 6.8, 1.6 Hz, 1H), 7.65 (d, $J$ = 8.0 Hz, 1H), 7.39 (t, $J$ = 7.2 Hz, 1H), 5.79 (s, 2H), 4.33 (d, $J$ = 5.6 Hz, 4H), 4.25 (d, $J$ = 5.6 Hz, 2H), 2.82 (m, 1H); $^{13}$C NMR (100 MHz, DMSO-$d_6$): $\delta$ 168.29, 163.85, 151.10, 149.15, 144.54, 142.46, 131.33, 130.67, 128.22, 127.58, 101.70, 72.99, 71.39, 38.56; HRMS (*m*/*z*): $[M+H]^+$ calcd for $C_{22}H_{22}N_7O_9$, 528.15; found, 528.15.

### 4.11. 1-[*O*-(6-Uracilcarboxaldoximyl)]-3-[*O*-(3-carboxybenzaldoximyl)]-propane (50)

The synthesis and characterization of this oxime heterodimer has been previously described[33].

### 4.12. 2-{*O*-[2-(N1-uracil)-acetaldoximyl]-methyl}-1,3-bis[*O*-(3,4-dihydroxy-5-methoxybenzaldoximyl)]-propane (51)

$^1$H NMR (400 MHz, DMSO-$d_6$) $\delta$ 11.32 (d, 2H), 9.14 (s, 1H), 8.72 (s, 1H), 8.03 (q, 1H), 7.65 (dd, 1H), 7.56 (d, 1H), 7.52 (dd, 1H), 6.92 (dd, 1H), 6.69 (s, 1H), 5.55 (d, 2H), 4.50 (dd, 2H), 4.43 (t, 2H), 4.17–4.00 (m, 6H), 3.70 (s, 3H), 1.28 (m, 1H); $^{13}$C NMR (400 MHz, DMSO-$d_6$) $\delta$ (164.5, 164.4), 153.2, (151.8, 151.5), (150.8, 150.0), (149.1, 147.2), (146.5, 146.3), 143.5, 137.1, 122.7, 108.6, 103.2, (101.9, 101.8), 72.4, 72.0, 59.9, (56.9, 56.5), (46.5, 45.2); HRMS (*m*/*z*): $[M+H]^+$ calcd for $C_{24}H_{28}N_7O_{10}$ 574.1892, found 574.1885.

### 4.13. 2-[*O*-(3,4-Dihydroxy-5-methoxybenzaldoximyl)-methyl]-1,3-bis{*O*-[2-(N1-uracil)-acetaldoximyl]}-propane (52)

$^1$H NMR (400 MHz, DMSO-$d_6$) $\delta$ 11.33 (d, 1H), 9.14 (s, 2H), 8.72 (s, 2H), 8.03 (d, 2H), 7.65 (d, 0.5H), 7.56 (d, 0.5H), 7.53 (t, 0.5H), 6.93 (t, 0.5H), 6.69 (s, 2H), 5.55 (d, 1H), 4.50 (d, 1H), 4.43 (d, 1H), 4.42-4.00 (m, 6H), 3.70 (s, 6H), 1.24 (m, 1H); $^{13}$C NMR (400 MHz, DMSO-$d_6$) $\delta$ (164.5, 164.4), 153.2, (151.8, 151.5), (150.8, 150.0), (149.1, 147.2), (146.5, 146.3), 143.5, 137.1, 122.7, 108.7, 103.1, (101.9, 101.8), 72.4, 71.9, 59.9, (56.9, 56.4), (46.5, 45.2); HRMS (*m*/*z*): $[M+H]^+$ calcd for $C_{26}H_{30}N_5O_{11}$ 588.1936, found 588.1920.

## 5. In vitro inhibition studies

### 5.1. High-throughput inhibitor screening of UDG

The molecular beacon-based HTS assay for UDG has been previously described.[33] Briefly, to a 96-well microtiter plate was added 5 μL of 2 mM total compound in DMSO, followed by 75 μL 33.3 pM human UNG in reaction buffer (10 mM Tris–HCl, pH 8.0, 20 mM NaCl, 7.5 mM $MgCl_2$, 0.002% brij-35). The reactions were initiated by the addition of 20 μL of 250 nM molecular beacon substrate in reaction buffer. The plates are incubated at ambient temperature in a fluorescence plate reader for 30 min, and the progress of the reaction was monitored every 5 min (Ex. 485 nm/Em. 520 nm). The final concentrations of the reagents in the assay are 10 mM Tris–HCl, pH 8.0, 20 mM NaCl, 7.5 mM $MgCl_2$, 0.002% Brij-35, 25 or 100 pM human UNG, 50 nM molecular beacon substrate, 100 μM total compound, and 5% DMSO. $IC_{50}$ analysis was performed using the same conditions except that the concentration of compound was varied in the range 0.01–100 μM.

### 5.2. High-throughput inhibitor screening of dUTPase

To a 96-well microtiter plate were added 20 μL of reaction buffer (50 mM Tris, pH 8.0, 10 mM $MgCl_2$, and 0.05% Tween 20) and 5 μL of compounds (2 mM) in DMSO, followed by 50 μL of dUTPase (1 nM) and pyrophosphatase (10 U/mL) in reaction buffer. The reactions were initiated by the addition of 25 μL dUTP (40 μM). The plates are incubated at ambient temperature for 50 min and the reactions were quenched by 25 μL of malachite green color reagent.[45] The mixtures were then allowed to stand for 10 min and the absorbances were measured using a microtiter plate reader with a 620 nm bandpass filter. $IC_{50}$ analysis was performed using the same conditions except that the concentration of compound was varied in the range 0.1–75 μM.

## Acknowledgments

This work was supported by NIH Grant GM56834-10 to J.T.S. D.J.K. was supported by the DOD Breast Cancer Research Program (DAMD17-03-1-1251).

## Supplementary data

Tables of aryl aldehydes and hydroxybenzaldehydes used to construct oxime libraries, NMR confirmation of product ratios for representative oximes, and $IC_{50}$ curves for active compounds. Supplementary data associated with this article can be found, in the online version, at doi:10.1016/j.bmc.2006.04.022.

## References and notes

1. Lindahl, T.; Wood, R. D. *Science* **1999**, *286*, 1897–1905.
2. Unniraman, S.; Fugmann, S. D.; Schatz, D. G. *Science* **2004**, *305*, 1113–1114.
3. Seiple, L.; Jaruga, P.; Dizdaroglu, M.; Stivers, J. T. *Nucleic Acids Res.* **2006**, *34*, 140–151.
4. Saribasak, H.; Saribasak, N. N.; Ipek, F. M.; Ellwart, J. W.; Arakawa, H.; Buerstedde, J. M. *J. Immunol.* **2006**, *176*, 365–371.
5. Tye, B. K.; Lehman, I. R. *J. Mol. Biol.* **1977**, *117*, 293–306.

6. Warner, H. R.; Duncan, B. K. *Nature* **1978**, *272*, 32–34.
7. Nilsen, H.; Haushalter, K. A.; Robins, P.; Barnes, D. E.; Verdine, G. L.; Lindahl, T. *EMBO J.* **2001**, *20*, 4278–4286.
8. Di Noia, J.; Neuberger, M. S. *Nature* **2002**, *419*, 43–48.
9. Imai, K.; Slupphaug, G.; Lee, W. I.; Revy, P.; Nonoyama, S.; Catalan, N.; Yel, L.; Forveille, M.; Kavli, B.; Krokan, H. E.; Ochs, H. D.; Fischer, A.; Durandy, A. *Nat. Immunol.* **2003**, *4*, 1023–1028.
10. Storb, U.; Stavnezer, J. *Curr. Biol.* **2002**, *12*, R725–R727.
11. Chen, R.; Wang, H.; Mansky, L. M. *J. Gen. Virol.* **2002**, *83*, 2339–2345.
12. Prichard, M. N.; Duke, G. M.; Mocarski, E. S. *J. Virol.* **1996**, *70*, 3018–3025.
13. De Silva, F. S.; Moss, B. *J. Virol.* **2003**, *77*, 159–166.
14. Stuart, D. T.; Upton, C.; Higman, M. A.; Niles, E. G.; McFadden, G. *J. Virol.* **1993**, *67*, 2503–2512.
15. Priet, S.; Gros, N.; Navarro, J. M.; Boretto, J.; Canard, B.; Querat, G.; Sire, J. *Mol. Cell* **2005**, *17*, 479–490.
16. Ladner, R. D. *Curr. Protein Pept. Sci.* **2001**, *2*, 361–370.
17. Tinkelenberg, B. A.; Hansbury, M. J.; Ladner, R. D. *Cancer Res.* **2002**, *62*, 4909–4915.
18. Stivers, J. T.; Drohat, A. C. *Arch. Biochem. Biophys.* **2001**, *396*, 1–9.
19. Bouhamdan, M.; Benichou, S.; Rey, F.; Navarro, J. M.; Agostini, I.; Spire, B.; Camonis, J.; Slupphaug, G.; Vigne, R.; Benarous, R.; Sire, J. *J. Virol.* **1996**, *70*, 697–704.
20. BouHamdan, M.; Xue, Y.; Baudat, Y.; Hu, B.; Sire, J.; Pomerantz, R. J.; Duan, L. X. *J. Biol. Chem.* **1998**, *273*, 8009–8016.
21. Chen, R.; Le Rouzic, E.; Kearney, J. A.; Mansky, L. M.; Benichou, S. *J. Biol. Chem.* **2004**, *279*, 28419–28425.
22. Klarmann, G. J.; Chen, X.; North, T. W.; Preston, B. D. *J. Biol. Chem.* **2003**, *278*, 7902–7909.
23. Mansky, L. M.; Preveral, S.; Selig, L.; Benarous, R.; Benichou, S. *J. Virol.* **2000**, *74*, 7039–7047.
24. Payne, S. L.; Elder, J. H. *Curr. Protein Pept. Sci.* **2001**, *2*, 381–388.
25. Selig, L.; Benichou, S.; Rogel, M. E.; Wu, L. I.; Vodicka, M. A.; Sire, J.; Benarous, R.; Emerman, M. *J. Virol.* **1997**, *71*, 4842–4846.
26. Willetts, K. E.; Rey, F.; Agostini, I.; Navarro, J. M.; Baudat, Y.; Vigne, R.; Sire, J. *J. Virol.* **1999**, *73*, 1682–1688.
27. Elder, R. T.; Zhu, X.; Priet, S.; Chen, M.; Yu, M.; Navarro, J. M.; Sire, J.; Zhao, Y. *Biochem. Biophys. Res. Commun.* **2003**, *306*, 693–700.
28. Mansky, L. M.; Le Rouzic, E.; Benichou, S.; Gajary, L. C. *J. Virol.* **2003**, *77*, 2071–2080.
29. Miller, R. J.; Cairns, J. S.; Bridges, S.; Sarver, N. *J. Virol.* **2000**, *74*, 7187–7195.
30. Lau, A.; Swinbank, K. M.; Ahmed, P. S.; Taylor, D. L.; Jackson, S. P.; Smith, G. C.; O'Connor, M. J. *Nat. Cell Biol.* **2005**, *7*, 493–500.
31. Nilsen, H.; Rosewell, I.; Robins, P.; Skjelbred, C. F.; Andersen, S.; Slupphaug, G.; Daly, G.; Krokan, H. E.; Lindahl, T.; Barnes, D. E. *Mol. Cell* **2000**, *5*, 1059–1065.
32. Maier, L.; Spoerri, H. Organic phosphorus compounds. 103. Aminooxyalkylphosphinic acids and aminooxyalkylphosphine oxides and derivatives. In *Phosphorus, Sulfur and Silicon and the Related Elements*, Ed.; Vol. 70; 1992; pp 49–57.
33. Jiang, Y. L.; Krosky, D. J.; Seiple, L.; Stivers, J. T. *J. Am. Chem. Soc.* **2005**, *127*, 17412–17420.
34. Jiang, Y. L.; Cao, C.; Stivers, J. T.; Song, F.; Ichikawa, Y. *Bioorg. Chem.* **2004**, *32*, 244–262.
35. Krosky, D. J.; Song, F.; Stivers, J. T. *Biochemistry* **2005**, *44*, 5949–5959.
36. Whittingham, J. L.; Leal, I.; Nguyen, C.; Kasinathan, G.; Bell, E.; Jones, A. F.; Berry, C.; Benito, A.; Turkenburg, J. P.; Dodson, E. J.; Ruiz Perez, L. M.; Wilkinson, A. J.; Johansson, N. G.; Brun, R.; Gilbert, I. H.; Gonzalez Pacanowska, D.; Wilson, K. S. *Structure* **2005**, *13*, 329–338.
37. Spigset, O.; Granberg, K.; Hagg, S.; Soderstrom, E.; Dahlqvist, R. *Br. J. Clin. Pharmacol.* **1998**, *45*, 257–263.
38. Hemeryck, A.; Belpaire, F. M. *Curr. Drug Metab.* **2002**, *3*, 13–37.
39. Sturk, L. M.; Brock, J. L.; Bagnell, C. R.; Hall, J. E.; Tidwell, R. R. *Acta Trop.* **2004**, *91*, 131–143.
40. Heberling, S.; Girreser, U.; Wolf, S.; Clement, B. *Biochem. Pharmacol.* **2006**, *71*, 354–365.
41. Kurian, J. R.; Bajad, S. U.; Miller, J. L.; Chin, N. A.; Trepanier, L. A. *J. Pharmacol. Exp. Ther.* **2004**, *311*, 1171–1178.
42. Maly, D. J.; Choong, I. C.; Ellman, J. A. *Proc. Natl. Acad. Sci. U.S.A.* **2000**, *97*, 2419–2424.
43. Kung, P. P.; Bharadwaj, R.; Fraser, A. S.; Cook, D. R.; Kawasaki, A. M.; Cook, P. D. *J. Org. Chem.* **1998**, *63*, 1846–1852.
44. Weiss, R. H.; Furfine, E.; Hausleden, E.; Dixon, D. W. *J. Org. Chem.* **1984**, *49*, 4969–4972.
45. Geladopoulos, T. P.; Sotiroudis, T. G.; Evangelopoulos, A. E. *Anal. Biochem.* **1991**, *192*, 112–116.